Casimir Forces and Quantum Electrodynamical Torques: Physics and Nanomechanics

Federico Capasso, *Fellow, IEEE*, Jeremy N. Munday, Davide Iannuzzi, *Member, IEEE*, and H. B. Chan

(Invited Paper)

***Abstract*—This paper discusses recent developments on quantum electrodynamical (QED) phenomena, such as the Casimir effect, and their use in nanomechanics and nanotechnology in general. Casimir forces and torques arise from quantum fluctuations of vacuum or, more generally, from the zero-point energy of materials and their dependence on the boundary conditions of the electromagnetic fields. Because the latter can be tailored, this raises the interesting possibility of designing QED forces for specific applications. After a concise review of the field in an historical perspective, high precision measurements of the Casimir force using microelectromechanical systems (MEMS) technology and applications of the latter to nonlinear oscillators are presented, along with a discussion of its use in nanoscale position sensors. Then, experiments that have demonstrated the role of the skin-depth effect in reducing the Casimir force are presented. The dielectric response of materials enters in a nonintuitive way in the modification of the Casimir–Lifshitz force between dielectrics through the dielectric function at imaginary frequencies $\varepsilon(i\xi)$. The latter is illustrated in a dramatic way by experiments on materials that can be switched between a reflective and a transparent state (hydrogen switchable mirrors). Repulsive Casimir forces between solids separated by a fluid with $\varepsilon(i\xi)$ intermediate between those of the solids over a large frequency range is discussed, including ongoing experiments aimed at its observation. Such repulsive forces can be used to achieve quantum floatation in a virtually frictionless environment, a phenomenon that could be exploited in innovative applications to nanomechanics. The last part of the paper deals with the elusive QED torque between birefringent materials and efforts to observe it. We conclude by highlighting future important directions.**

***Index Terms*—Casimir effect, electromagnetic properties, MEMS, microelectromechanical devices, quantum electrodynamics (QED), van der Waals forces.**

Manuscript received December 1, 2006. This work was supported in part by the Nanoscale Science and Engineering Center (NSEC) under NSF Contract PHY-0117795 and in part by the Center for Nanoscale Systems at Harvard University. The work of J. N. Munday was supported by the NSF Graduate Research Fellowship Program (GRFP). The work of D. Iannuzzi was supported by the Netherlands Organization for Scientific Research (NWO) through the Innovational Research Incentives Scheme Vernieuwingsimpuls VIDI-680-47-209. The work of H. B. Chan was supported by the Department of Energy under Grant DE-FG02-05ER46247.

F. Capasso is with the Harvard School of Engineering and Applied Sciences, Harvard University, Cambridge, MA 02138 USA (e-mail: capasso@deas.harvard.edu).

J. N. Munday is with the Department of Physics, Harvard University, Cambridge, MA 02138 USA (e-mail: munday@fas.harvard.edu).

D. Iannuzzi is with the Condensed Matter Physics, Division of Physics and Astronomy, Vrije Universiteit, 1081 HV Amsterdam, The Netherlands (e-mail: iannuzzi@few.vu.nl).

H. B. Chan is with the Department of Physics, University of Florida, Gainesville, FL 32611 USA (e-mail: hochan@phys.ufl.edu).

Digital Object Identifier 10.1109/JSTQE.2007.893082

I. Introduction

NANOMECHANICS is a rapidly developing research frontier where basic physics and high technology converge, opening the door to exciting and possibly revolutionary applications [1]–[4]. One goal is the observation of a variety of quantum regimes on a mesoscopic scale; a case in point is the discovery of the quantization of thermal conductance in nanoelectromechanical systems (NEMS) [5] or the current effort in reaching the Heisenberg limit of momentum and position measurements in mechanical oscillators [6]–[8].

A variety of exotic quantum electrodynamical (QED) phenomena can be observed when metallic and dielectric surfaces are placed in close proximity (< 100 nm). This opens the door to intriguing opportunities, particularly in the field of nanomechanics.

According to QED, quantum fluctuations of the electromagnetic field give rise to a zero-point energy that never vanishes, even in empty space [9]. In 1948, Casimir [10] showed that, as a consequence, two parallel plates, made out of ideal metal (i.e., with unity reflectivity at all wavelengths, or equivalently with infinite plasma frequency), should attract each other in vacuum even if they are electrically neutral, a phenomenon known as the Casimir effect. Because only the electromagnetic modes that have nodes on both walls can exist within the cavity, the zero-point energy depends on the separation between the plates, giving rise to an attractive force. This result, in fact, can be interpreted as due to the differential radiation pressure associated with zero-point energy (virtual photons) between the "inside" and the "outside" of the plates, which leads to an attraction because the mode density in free space is higher than the density of states between the plates [9]. The interpretation in terms of zero-point energy of the Casimir effect was suggested by Niels Bohr, according to Casimir's autobiography [11]. An equivalent derivation of excellent intuitive value, leading to the Casimir force formula, was recently given by Jaffe and Scardicchio in terms of virtual photons moving along ray optical paths [12], [13].

Between two parallel plates, the Casimir force assumes the form [10]

$$F_c = \frac{-\pi^2 \hbar c A}{240 d^4} \tag{1}$$

where c is the speed of light, $\hbar$ is Planck constant divided by 2π, A is the area of the plates, and d is their separation.

The pioneering experiments of Sparnaay [14] were not able to unambiguously confirm the existence of the Casimir force

due to, among other factors, the large error arising form the difficulty in maintaining a high degree of parallelism between the plates (1). Clear experimental evidence for the effect was presented by van Blokland and Overbeek in 1978, who performed measurements between a sphere and a plate [15], thus eliminating a major source of uncertainty. Final decisive verification is due to Lamoureaux, who in 1997 reported the first high precision measurements of the Casimir force using a torsional pendulum and sphere–plate configuration [16]. This was followed by several experimental studies, which have produced further convincing confirmation [17]–[24] for the Casimir effect including the parallel plate geometry [21].

Between a sphere and a plate made of ideal metals, the Casimir force reads [25]

$$F_c = \frac{-\pi^3 \hbar c R}{360 d^3} \tag{2}$$

where R is the radius of the sphere and d is the minimum distance between the sphere and the plate. In the derivation of (2), it was assumed that this distance is much smaller than the sphere diameter.

Several reviews on Casimir forces and on the closely related van der Waals forces have recently appeared [26]–[34].[1] Both forces are of QED origin. The key physical difference is that in the Casimir case, retardation effects due to the finite speed of light cannot be neglected, as in the van der Waals limit, and are actually dominant [9]. This is true for distances so that the propagation time of light between the bodies or two molecules is much greater than the inverse characteristic frequency of the material or of the molecules (for example, the inverse plasma frequency in the case of metals and the inverse of the frequency of the dominant transition contributing to the polarizabity $\alpha(\omega)$, in the case of molecules) [9]. The complete theory for macroscopic bodies, developed by Lifshitz, Dzyaloshinskii, and Pitaevskii, is valid for any distance between the surfaces of the latter and includes, in a consistent way, both limits [35], [36].

This formulation, a generalization of Casimir's theory to dielectrics, including of course nonideal metals, is the one that is most often used for comparison with experiments. In this theory, the force between two uncharged surfaces can be derived according to an analytical formula (often called the Lifshitz formula) that relates the zero-point energy to the dielectric functions of the interacting surfaces and of the medium in which they are immersed. This equation for the force between a sphere and a plate of the same metal is [35]

$$F_1(z) = \frac{\hbar}{2\pi c^2} R \int_0^\infty \int_1^\infty p\xi^2 \left\{ \ln\left[1 - \frac{(s-p)^2}{(s+p)^2} e^{-2pz\xi/c}\right] + \ln\left[1 - \frac{(s-p\varepsilon)^2}{(s+p\varepsilon)^2} e^{-2pz\xi/c}\right] \right\} dp\, d\xi \tag{3}$$

where $s = \sqrt{\varepsilon - 1 + p^2}$, $\varepsilon(i\xi)$ is the dielectric function of the dielectric or metal evaluated at imaginary frequency $i\xi$, and the integration is over all frequencies and wave vectors of the modes between the plates. The expression for $\varepsilon(i\xi)$ is given by

$$\varepsilon(i\xi) = 1 + \frac{2}{\pi} \int_0^\infty \frac{\omega \varepsilon''(\omega)}{\omega^2 + \xi^2}\, d\omega \tag{4}$$

where $\varepsilon''(\omega)$ is the imaginary part of the dielectric function. The integral in (4) runs over all real frequencies, with nonnegligible contributions arising from a very wide range of frequencies. Equations (3) and (4) show that the optical properties of the material influence the Casimir force in a nonintuitive way. The finite conductivity modifications to the Casimir force based on the frequency dependence of the dielectric function can be calculated numerically using the tabulated complex dielectric function of the metal [37]–[41]. This leads to a reduction in the Casimir force compared to the ideal metal case given by (1). Physically, this can be understood from the fact that, in a real metal, the electromagnetic field penetrates by an amount of the order of the skin-depth that leads to an effective increase of the plate separation.

The second modification, due to the roughness of the metallic surfaces, tends to increase the attraction [42]–[44] because the portions of the surfaces that are locally closer contribute much more to the force due its strong nonlinearity with distance.

As previously mentioned, at very short distances, the theory of Lifshitz, Dzyaloshinskii, and Pitaevskii also provides a complete description of the nonretarded van der Waals force [45], [46]. Recently, Henkel *et al*. [47] and Intravaia and Lambrecht [48] have provided a physically intuitive description of the van der Waals limit for real metals with dispersion described by the Drude model. At finite plasma frequency, one must include surface plasmons in the counting of electromagnetic modes, i.e., modes associated with surface charge oscillations that exponentially decay away from the surface. At short distances (small compared to the plasma wavelength), the Casimir energy is given by the shift in the zero-point energy of the surface plasmons due to their Coulomb (electrostatic) interaction. The corresponding attractive force between two parallel plates is, then, given by [49]

$$F_c = -\frac{\hbar c \pi^2 A}{290 \lambda_p d^3}. \tag{5}$$

This formula is an approximation of the short distance limit of the more complete theory [35], [36].

At large separations ($d \gg \lambda_p$), retardation effects give rise to a long-range interaction that, in the case of two ideal metals in vacuum, reduces to Casimir's result.

In a number of studies, several authors [19], [22], [23] have claimed agreement between Casimir force experiments and theory at the 1% level or better—a claim that has been challenged in some of the literature [20], [50]–[52]. The authors of [52] have pointed out that the strong nonlinear dependence of the force on distance limits the precision in the absolute determination of the force. Uncertainties in the knowledge of the dielectric functions of the thin metallic films used in the experiments and in the models of surface roughness used to correct the Lifshitz theory also typically give rise to errors larger than 1% in the calculation of the expected force [20], [51], [52]. It has also been shown that the calculation of the Casimir force can vary by as much as 5%

[1]For an extensive bibliography on the Casimir effect, see http://www.cfa.harvard.edu/∼babb/casimir-bib.html.

depending on which values are chosen for the optical properties of a given material [53]. Another uncertainty is related to the model of surface roughness and in its measurement that translates to an uncertainty in the comparison between theory and experiments. We conclude that claims of agreement between theory and experiment at the 1% level or less are questionable due to experimental errors and uncertainties in the calculations.

Apart from its intrinsic theoretical interest, the Casimir interaction has recently received considerable attention for its possible technological consequences. The Casimir force, which rapidly increases as the surface separation decreases, is the dominant interaction mechanism between neutral objects at submicron distances. In light of the miniaturization process that is moving modern technology toward smaller electromechanical devices, it is reasonable to ask what role the zero-point energy might play in the future development of micro- and nanoelectromechanical systems (MEMS and NEMS) [24], [54], [55]. The first experimental works related to this topic were performed at Bell Laboratories by two of the authors and their collaborators [24], [55].

The goal of their first experiment [24] was to design a micromachined torsional device that could be actuated solely by the Casimir force. The results not only demonstrated that this is, indeed, possible, but also provided one of the most sensitive measurements of the Casimir force between metallized surfaces. In their second experiment [55], the group showed that the Casimir attraction can also influence the dynamical properties of a micromachined device, changing its resonance frequency and giving rise to hysteretic behavior and bistability in its frequency response to an ac excitation, as expected for a nonlinear oscillator. They proposed that this device could serve as a nanometric position sensor. The aforementioned developments are covered in Section II.

A particularly interesting direction of research on Casimir–Lifshitz forces is the possibility of designing their strength and spatial dependence by a suitable control of the boundary conditions of the electromagnetic fields. This can be done by an appropriate choice of the materials [56], of the thickness of the metal films [57], and of the shape of the interacting surfaces [58]–[60]. By coating one of the surfaces with suitably engineered thin films, the influence of visible and infrared virtual photons in the Casimir interaction and the role of the skin-depth effect in Casimir forces can be explored, as discussed in Section III.

Section III also covers one of the most interesting features of long-range QED forces: the possibility of repulsive forces that can arise between suitable surfaces when their dielectric functions and that of the medium separating them satisfy a particular inequality [36], [45], [46]. Methods of measuring these forces and the phenomenon of "quantum floatation" are discussed along with intriguing applications to nanotechnology such as frictionless bearings and related devices.

QED can give rise to other exotic macroscopic interaction phenomena between materials with anisotropic optical properties such as birefringent crystals. For example, a torque due to quantum fluctuations between plates made of uniaxial materials has been predicted but has not yet been observed [61], [62]. Section IV is devoted to a discussion of this remarkable effect and related calculations. Specific experiments are proposed along with novel applications. Section V provides an outlook on novel directions in this field.

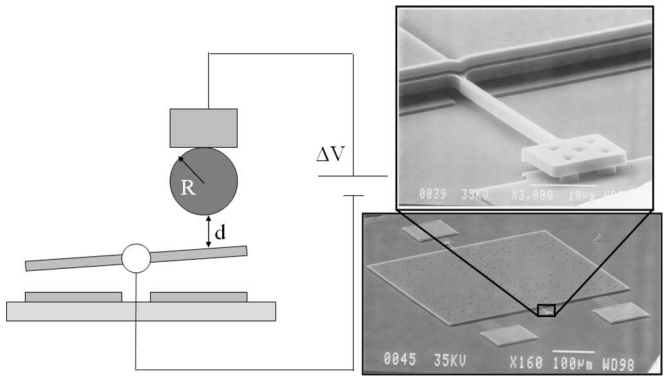

Fig. 1. MEMS Casimir force detection setup. Schematic of the experiment (not to scale) and scanning electron micrographs of the micromachined torsional device used for the measurement of the Casimir force with a closeup of one of the torsional rods anchored to the substrate. As the metallic sphere approaches the top plate, the Casimir force causes a rotation of the torsional rod.

II. MEMS Based on the Casimir Force

MEMS are a silicon-based integrated circuit technology with moving mechanical parts that are released by means of etching sacrificial silicon dioxide layers followed by a critical point drying step [63]. They have been finding increasing applications in several areas ranging from actuators and sensors to routers for optical communications. For example, the release of the airbag in cars is controlled by a MEMS-based accelerometer. In the area of lightwave communications, the future will bring about new optical networks with a mesh topology, based on dense wavelength division multiplexing. These intelligent networks will be adaptive and self-healing with capabilities of flexible wavelength provisioning, i.e., the possibility to add and drop wavelengths at specific nodes in response to real-time bandwidth demands and rerouting. The *lambda router* [64], [65], a device consisting of an array of thousands of voltage-controlled mirrors, which switches an incoming wavelength from one optical fiber to any of many output fibers, is an example of a potentially disruptive MEMS technology that might impact future networks.

The development of increasingly complex MEMS will lead to more attention to scaling issues, as this technology evolves toward NEMS. Thus, it is conceivable that a Moore curve for MEMS will develop leading to increasingly complex and compact MEMS having more devices in close proximity [66], [67]. This scenario will inevitably lead to having to face the issue of Casimir interactions between metallic and dielectric surfaces in close proximity with attention to potentially troublesome phenomena such as stiction, i.e., the irreversible coming into contact of moving parts due to Casimir/van der Waals forces [66]. On the other hand, such phenomena might be usable to one's advantage by adding functionality to NEMS-based architectures.

A. Actuators

In the first experiment [24], the authors designed and demonstrated a micromachined torsional device that was actuated by

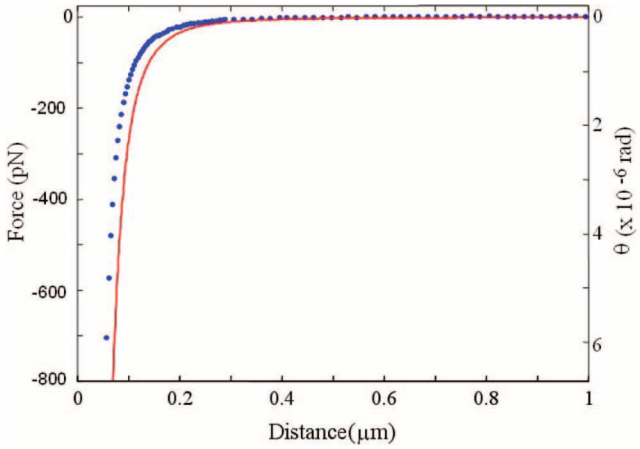

Fig. 2. Experimental measurement of the Casimir force from the MEMS torsional apparatus. Angle of rotation of the top plate in response to the Casimir force as a function of distance. (Red line) Predicted Casimir force (2) without corrections for surface roughness or finite conductivity. (Blue Dots) Experimental results.

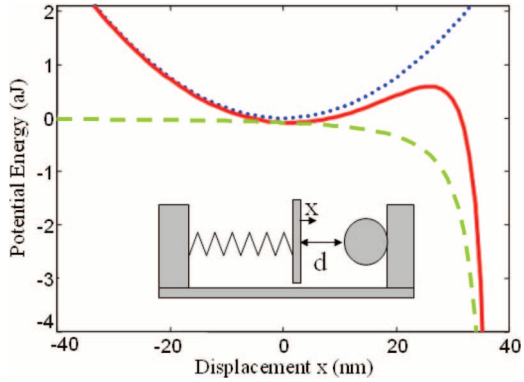

Fig. 3. Simple model of the nonlinear Casimir oscillator (not to scale) (inset). Elastic potential energy of the spring (dotted line, spring constant 0.019 Nm^{-1}), energy associated with the Casimir attraction (dashed line), and total potential energy (solid line) as a function of plate displacement. The distance d between the sphere (100 μm radius) and the equilibrium position of the plate in the absence of the Casimir force is chosen to be 40 nm.

the Casimir force and that provided a very sensitive measurement of the latter. This device (Fig. 1) was subsequently used in a variety of experiments [22], [57], [68]. It consists of a 3.5-μm-thick, 500-μm-square heavily doped polysilicon plate freely suspended on two of its opposite sides by thin torsional rods. The other ends of the torsional rods are anchored to the substrate via support posts. Two fixed polysilicon electrodes are located symmetrically underneath the plate, one on each side of the torsional rod. Each electrode is half the size of the top plate. There is a 2 μm gap between the top plate and the fixed electrodes created by etching a SiO_2 sacrificial layer. The top plate is, thus, free to rotate about the torsional rods in response to an external torque.

A schematic of the actuation mechanism based on the Casimir force is shown in Fig. 1. A polystyrene sphere with radius $R = 100$ μm is glued at the end of a copper wire using conductive epoxy. A 200-nm-thick film of gold with a thin titanium adhesion layer is evaporated on both the sphere and the top plate of the torsional device. An additional 10 nm of gold is sputtered on the sphere to provide electrical contact to the wire. The micromachined device is placed on a piezoelectric translation stage with the sphere positioned close to one side of the top plate. As the piezo extends, it moves the micromachined device toward the sphere. The rotation of the top plate in response to the attractive Casimir force is detected by measuring the imbalance of the capacitances of the top plate to the two bottom electrodes at different separations between the sphere and the top plate. The measurement is performed at room temperature and at a pressure of less than 1 mtorr. Note that an external bias needs to be applied to the sphere to compensate for the patch potential V_0 resulting from work function differences between the metallic surfaces and other effects such as contact potentials associated with grounding, etc. [15]. The value of V_0 is typically in the range of 10–100 mV.

Fig. 2 shows the results of that measurement. One sees that the data points lie above the curve given by (2). Two main effects are at work in this discrepancy. The first one is the finite reflectivity of any metal. This causes virtual photons associated with vacuum fluctuations to penetrate into the metal (skin effect) increasing the effective sphere–plate separation, thus decreasing the force. The second effect is the surface roughness estimated from atomic force microscope (AFM) measurements to be a few tens of nanometers depending on the particulars of the experiment. It enhances the Casimir force due to the strong nonlinear dependence with distance. Both effects can be accounted for within the framework of Lifshitz theory, giving a much smaller discrepancy between theory and experiments [52].

A bridge circuit enables one to measure the change in capacitance to 1 part in 2×10^5, equivalent to a rotation angle of 8×10^{-8} rad, with integration time of 1 s when the device is in vacuum. With a torsional spring constant as small as 1.5×10^{-8}Nm rad^{-1}, the device yields a sensitivity of 5 pN $\mathrm{Hz}^{-1/2}$ for forces acting at the edge of the plate. Such force sensitivity is comparable to the resolution of conventional AFMs. The device is insensitive to mechanical noise from the surroundings because the resonant frequency is maintained high enough ($\sim$2 kHz) due to the small moment of inertia of the plate.

B. Nonlinear Oscillators

While there is vast experimental literature on the hysteretic response and bistability of nonlinear oscillators in the context of quantum optics, solid state physics, mechanics, and electronics, the experiment summarized in this section represents, to our knowledge, the first observation of bistability and hysteresis caused by a QED effect. A simple model of the Casimir oscillator consists of a movable metallic plate subjected to the restoring force of a spring obeying Hooke's law and the nonlinear Casimir force arising from the interaction with a fixed metallic sphere (Fig. 3). For separations d larger than a critical value [69], the system is bistable: the potential energy consists of a local minimum and a global minimum separated by a potential barrier (Fig. 3). The local minimum is a stable equilibrium position, about which the plate undergoes small oscillations. The Casimir force modifies the curvature of the confining potential

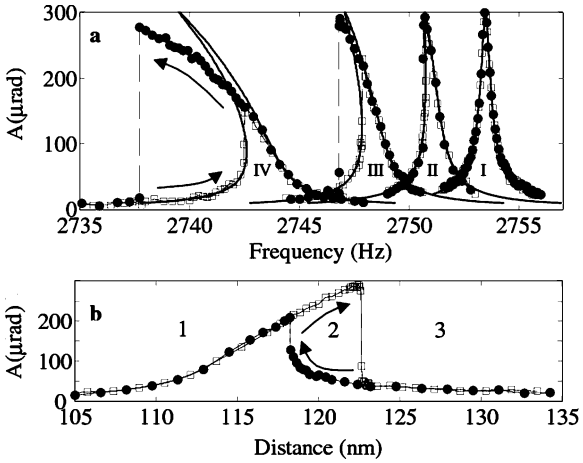

Fig. 4. (a) Hysteresis in the frequency response induced by the Casimir force on an otherwise linear oscillator. Hollow squares (solid circles) are recorded with increasing (decreasing) frequency. (Solid lines) The predicted frequency response of the oscillator. The distance d between the oscillator and the sphere is 3.3 μm, 141 nm, 116.5 nm, and 98 nm for peaks I, II, III, and IV, respectively. The excitation amplitude is maintained constant at 55.5 mV for all four separations. The solid lines are the calculated response. The peak oscillation amplitude for the plate is 39 nm at its closest point to the sphere. (b) Oscillation amplitude as a function of distance with excitation frequency fixed at 2748 Hz.

around the minimum, thus changing the natural frequency of oscillation, and also introduces higher order terms in the potential, making the oscillations anharmonic.

For this experiment, the same device as in Fig. 1 was used. The torsional mode of oscillation was excited by applying a driving voltage to one of the two electrodes that is fixed in position under the plate. The driving voltage is a small ac excitation $V_{\rm ac}$ with a dc bias $V_{\rm dc1}$ to linearize the voltage dependence of the driving torque. The top plate is grounded while the detection electrode is connected to a dc voltage $V_{\rm dc2}$ through a resistor. Oscillatory motion of the top plate leads to a time-varying capacitance between the top plate and the detection electrode. For small oscillations, the change in capacitance is proportional to the rotation of the plate. The detection electrode is connected to an amplifier and a lock-in amplifier measures the output signal at the excitation frequency.

To demonstrate the nonlinear effects introduced by the Casimir force, the piezo was first retracted until the sphere was more than 3.3 μm away from the oscillating plate so that the Casimir force had a negligible effect on the oscillations. The measured frequency response shows a resonance peak that is characteristic of a driven harmonic oscillator (peak I in Fig. 4(a)), regardless of whether the frequency is swept up (hollow squares) or down (solid circles). This ensures that the excitation voltage is small enough so that intrinsic nonlinear effects in the oscillator are negligible in the absence of the Casimir force. The piezo was, then, extended to bring the sphere close to the top plate while maintaining the excitation voltage at fixed amplitude. The resonance peak shifts to lower frequencies (peaks II, III, and IV) by an amount that is consistent with the distance dependence of the force in Fig. 2. Moreover, the shape of the resonance peak deviates from that of a driven harmonic oscillator and becomes asymmetric. As the distance decreases, the asymmetry becomes stronger and hysteresis occurs. This reproducible hysteretic behavior is characteristic of strongly nonlinear oscillations [70].

The solid lines in Fig. 4(a) show the predicted frequency response of the oscillator including the first, second, and third spatial derivatives of the Casimir force. Higher orders terms or the full nonlinear potential would need to be included to achieve a better agreement with experiments.

An alternative way to demonstrate the "memory" effect of the oscillator is to maintain the excitation at a fixed frequency and vary the distance between the sphere and the plate (Fig. 4(b)). As the distance changes, the resonance frequency of the oscillator shifts to first order because of the changing force gradient. In region 1, the fixed excitation frequency is higher than the resonance frequency and vice versa for region 3. In region 2, the amplitude of oscillation depends on the history of the plate position. Depending on whether the plate was in region 1 or region 3 before it enters region 2, the amplitude of oscillation differs by up to a factor of 6. This oscillator, therefore, acts as a nanometric sensor for the separation between two uncharged metallic surfaces.

III. Design and Control of Casimir Forces

In this section, we discuss experiments aimed at tailoring the Casimir–Lifshitz force via control of the boundary conditions of the electromagnetic fields. Several examples will be discussed: (1) control of the thickness of the metallic layers deposited on the juxtaposed surfaces and (2) choice of materials that: (a) can be reversibly switched from metallic to transparent and (b) give rise to repulsive Casimir–Lifshitz force when separated by a suitable liquid.

A. Measurement of the Casimir Force Between Metallic Films: Skin-Depth Effect

The use of ultrathin metallic coatings (i.e., of thickness comparable to the skin-depth at wavelengths comparable to the distance between the surfaces) over transparent dielectrics, as opposed to thick layers, as employed in the experiments of Section II, should alter the distance dependence of the force.

At submicron distances, the Casimir force critically depends on the reflectivity of the interacting surfaces for wavelengths in the ultraviolet to far-infrared [35], [68]. The attraction between transparent materials is expected to be smaller than that between highly reflective mirrors as a result of a less effective confinement of electromagnetic modes inside the optical cavity defined by the surfaces. A thin metallic film can be transparent to electromagnetic waves that would otherwise be reflected by bulk metal. In fact, when its thickness is much less than the skin-depth, most of the light passes through the film. Consequently, the Casimir force between metallic films should be significantly reduced when its thickness is less than the skin-depth at ultraviolet to infrared wavelengths. For most common metals, this condition is reached when the thickness of the layer is ~ 10 nm.

The technique presented in [68] was recently perfected in terms of the calibration method used and allowed the accurate measurement of the Casimir force for different metal film thickness on the sphere [57].

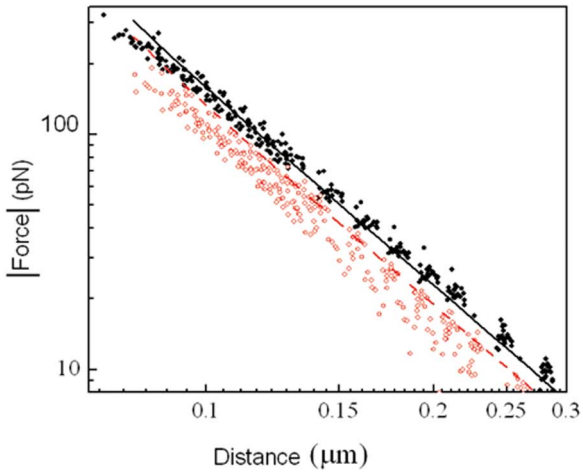

Fig. 5. Comparison between Casimir force measurements and calculations for a sphere–plate geometry. (Filled circles) Data obtained with a thick metallic film deposited on the sphere. (Open circles) Data for a thin film. (Continuous and dashed lines) Theoretical predictions for thick and thin films, respectively.

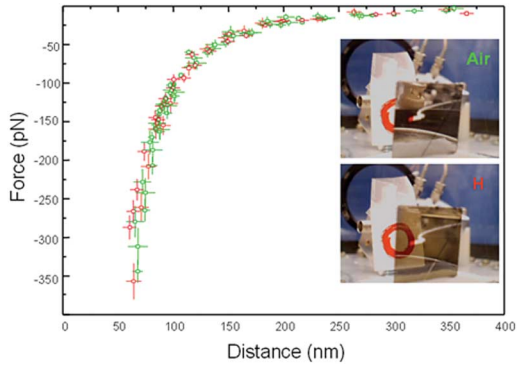

Fig. 6. Casimir force between a gold-coated plate and a sphere coated with a HSM as a function of the distance, in air (green dots) and in argon–hydrogen (red dots). HSM in air and in hydrogen (inset). A similar mirror was deposited on the sphere of our experimental apparatus.

Demonstrating the skin-depth effect requires careful control of the thickness and surface roughness of the films. The sphere was glued to its support and subsequently coated with a 2.92 nm titanium adhesion layer and a 9.23 nm film of palladium. The thickness of the titanium layer and the palladium film was measured by Rutherford backscattering on a silicon slice that was evaporated in close proximity to the sphere. After evaporation, the sphere was imaged with an optical profiler to determine its roughness, and mounted inside the experimental apparatus. After completion of the Casimir force measurements, the sphere was removed from the experimental apparatus, coated with an additional 200 nm of palladium, analyzed with the optical profiler, and mounted back inside the vacuum chamber for another set of measurements. It is important to stress that the surface roughness measured before and after the deposition of the thicker palladium layer was the same within a few percent.

In Fig. 5, the results of the thin-film measurements are compared with those obtained after the evaporation of the thick layer of palladium. The measurements were repeated 20 times for both the thin and thick films. The results clearly demonstrate the skin-depth effect on the Casimir force. The force measured with the thin film of palladium is, in fact, smaller than that observed after the evaporation of the thicker film. Measurements were repeated with a similar sphere: the results confirmed the skin-depth effect. To rule out possible spurious effects, the data were compared with a theoretical calculation (Fig. 5) based on the Lifshitz theory that includes the dielectric function of the metallic coatings and the effects of the surface roughness. The magnitude and spatial distribution of the latter was measured with an optical profilometer and incorporated in the modified Lifshitz equation [44], [57], [71]. The dielectric functions used in the calculation were obtained from [39]–[41] and [72], and a suitable modification of Lifshitz's theory to account for multiple thin films was used [45].

The discrepancy observed in the case of the thin metallic film is not surprising. The calculation of the force is based on two approximations: (1) the dielectric function for the metallic layers (both titanium and palladium) is assumed to be equal to the one tabulated for bulk-materials and (2) the model used to describe the dielectric function of polystyrene is limited to a simplified two-oscillator approximation [72]. These assumptions can lead to significant errors in the estimated force.

B. Hydrogen Switchable Mirrors

Using the experimental setup described in Section II, the Casimir force between a gold-coated plate and a sphere coated with a hydrogen switchable mirror (HSM) [73] was measured for separations in the 70–400 nm range [68]. The HSMs were obtained by repeating seven consecutive evaporations of alternate layers of magnesium (10 nm) and nickel (2 nm), followed by an evaporation of a thin film of palladium (5 nm). The inset of Fig. 6 shows a glass slide coated according to this procedure, both in its as-deposited state and in its hydrogenated state. It is evident that the optical properties of the film are very different in the two situations. The transparency of the film was measured over a wavelength range between 0.5 and 3 μm, and its reflectivity at $\lambda = 660$ nm, keeping the sample in air and in an argon–hydrogen atmosphere (4% hydrogen). The results are in good agreement with the values reported in [74].

The results of Casimir force measurements obtained in air and in a hydrogen-rich atmosphere are shown in Fig. 6. It is evident that the force does not change in a discernible way upon hydrogenation of the HSM [68].

In order to explain this apparently surprising result, one should first note that the dielectric properties of the HSMs used in this experiment are known only in a limited range of wavelengths, spanning approximately the range 0.3–2.5 μm [74]. However, because the separation between the sphere and the plate in the experiment is in the 100 nm range, one could expect that it is not necessary to know the dielectric function for $\lambda > 2.5$ μm, because those modes should not give rise to large contributions to the force. A mathematical analysis carried out using *ad hoc* models to describe the interacting surfaces has shown

that this is not necessarily the case. Because the Casimir force depends on the dielectric function at imaginary frequency (4) and the integral in the latter is over all frequencies, long wavelengths compared to the separation between the sphere and the plate can make a significant contribution to the force. Thus, one of the reasons for not having observed a change in the latter upon hydrogenation is likely related to the fact that that the imaginary part of the permittivity might not change significantly at long wavelengths. Recently, a more accurate analysis of the experiment [75] confirmed this result, but also added an important detail: for a correct comparison of data with theory, it is necessary to also take into account the presence of the 5-nm-thick palladium layer that was deposited on top of the HSMs to prevent oxidation and promote hydrogen absorption. Although this layer is fairly transparent to all wavelengths from ultraviolet to infrared, its contribution to the interaction reduces the expected change of the force by nearly a factor of 2. It is, thus, the combination of the effect of the reflectivity at long wavelengths and of the thin palladium film that limits the magnitude of the change of the force following hydrogenation. Still, calculations show that a small change in the Casimir force upon hydrogenation should be observable with improved experimental precision and with the use of HSMs of different composition [75].

C. Casimir Levitation

Modification of the Casimir force is of great interest from both a fundamental and an applied point-of-view. It is reasonable to ask whether such modifications can lead to repulsive forces in special cases. In 1968, Boyer showed that for a perfectly conducting spherical shell, the Casimir effect should give rise to an outward pressure [76]. Similar repulsive Casimir forces have also been predicted for cubic and rectangular cavities with specific aspect ratios [77], [78]. However, criticisms concerning these results have been raised [79] and, recently, the possibility of repulsive forces based on topology for a wide class of systems have been ruled out [80].

The possibility of topological repulsive Casimir forces, i.e., due to the confinement of quantum fluctuations of the electromagnetic fields in vacuum because of the geometrical structure of the interacting metallic bodies, is therefore controversial. In this section, we will describe a repulsive force that is strictly due to the optical properties of the materials involved. Such a mechanism is responsible for many phenomena in the nonretarded regime including the surface melting of solids [81] and the vertical ascent of liquid helium within a container (see, for example, the discussion in [28]).

The Casimir–Lifshitz force is always attractive between two identical materials; however, the force can become repulsive when two different materials are submerged in a third medium if their dielectric functions, evaluated at imaginary frequency, obey the following relationship [45], [46]:

$$\varepsilon_1(i\xi) < \varepsilon_3(i\xi) < \varepsilon_2(i\xi)$$

or

$$\varepsilon_2(i\xi) < \varepsilon_3(i\xi) < \varepsilon_1(i\xi) \tag{6}$$

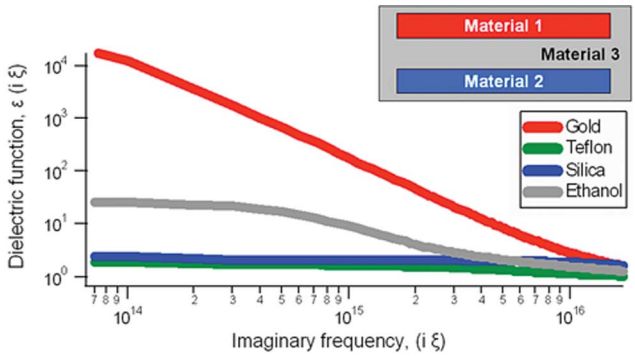

Fig. 7. Dielectric functions for four materials evaluated at imaginary frequency ($i\xi$). Schematic of the arrangement in which materials 1, 2, 3 are, respectively, gold, silica, and ethanol (*inset*). This sequence results in a repulsive Casimir–Lifshitz force between materials 1 and 2 because of the relative ordering of the dielectric functions: $\varepsilon_2(i\xi) < \varepsilon_3(i\xi) < \varepsilon_1(i\xi)$ at most frequencies.

TABLE I
HAMAKER CONSTANTS FOR VARIOUS MATERIAL COMBINATIONS

Materials (1-3-2)			Hamaker Constant
(1)	(3)	(2)	(10^{-20} J)
Gold	Ethanol	Silica	-2.46
Gold	Ethanol	Teflon AF®	-6.23
Gold	Ethanol	Polystyrene	-1.88
Gold	Water	Teflon AF®	-2.28
Aluminum	Ethanol	Silica	-1.57
Aluminum	Ethanol	Teflon AF®	-7.78
Aluminum	Ethanol	Polystyrene	-1.04
Aluminum	Water	Teflon AF®	-4.21

Calculated value of the Hamaker constant relative of the interaction between two macroscopic objects (materials 1 and 2) immersed in a liquid (material 3). The negative sign corresponds to repulsive force.

where ε_1 and ε_2 are the dielectric functions of the two outer materials and ε_3 is the dielectric function of the intervening material, as shown in the inset of Fig. 7. A repulsive interaction should be possible for many combinations of conventional materials as described later.

To give a more quantitative description of these forces, we have calculated the Hamaker constants as well as the full Casimir–Lifshitz force as a function of distance for several material combinations. The Hamaker constant A_{132} can be used to describe the magnitude and sign of the nonretarded (close range) van der Waals interaction between two objects (1 and 2) immersed in a third medium and depends on the dielectric functions of the materials involved [45], [82]. For instance, the van der Waals force between a sphere and a plate immersed in a liquid is given by$F = -A_{123}R/6d^2$, where R is the radius of the sphere and d is the separation between the sphere and the plate. Using this convention, a negative Hamaker constant corresponds to a positive, repulsive force. Table I shows the Hamaker constants for several material configurations, which should yield a repulsive interaction. Such materials were chosen because their dielectric functions obey (6) and are in common use for technological applications. The dielectric functions of these materials and of the intervening medium were obtained from [37]–[39] and [83]–[85]. For a complete description of the force at all distances, the full Lifshitz equation must be solved. This was done for a 100-μm-radius gold sphere above a silica

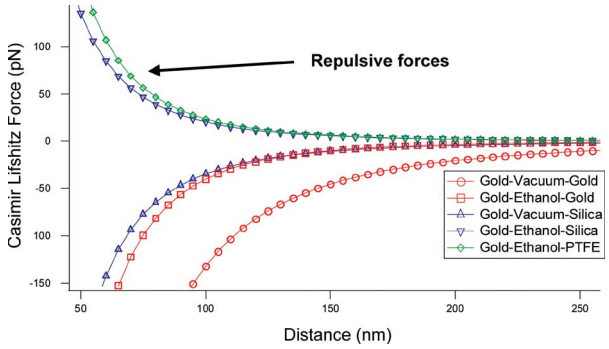

Fig. 8. Calculations of attractive and repulsive forces. The force calculations between gold and either silica or PTFE across vacuum or ethanol were obtained using the full Lifshiftz theory. Attractive forces have a negative sign for the force, while repulsive interactions have a positive sign.

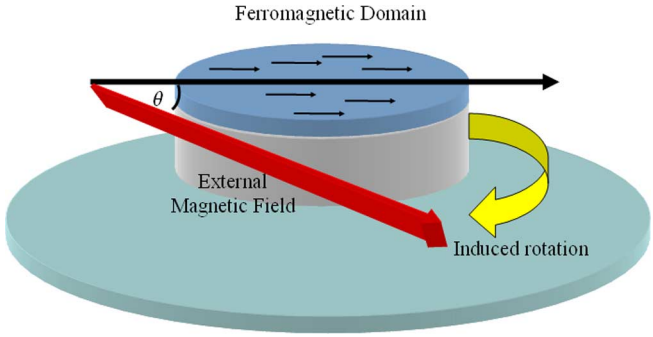

Fig. 9. QED floatation device. A repulsive force develops between the disk immersed in a fluid and the plate, which is balanced by gravity. We show a nano-compass that could be developed to mechanically sense small magnetic fields.

or polytetrafluoroethylene (PTFE, a generic form of Teflon) plate immersed in ethanol, as shown in Fig. 8. It can be seen from this figure that the combinations gold–ethanol–silica and gold–ethanol–PTFE give rise to a repulsive interaction while attractive interactions result when the intervening material is vacuum or when the two outer objects (1 and 2) are made of the same material.

Inequality (6) can also be used to predict the sign of the force. Fig. 7 shows $\varepsilon(i\xi)$ for gold, PTFE, silica, and ethanol (note that, for vacuum, $\varepsilon(i\xi) = 1$). From Figs. 7 and 8, also note that when inequality (6) is satisfied over a majority of frequencies, the interaction is repulsive and, when it is not satisfied, the interaction is attractive. For very high frequencies, the differences in $\varepsilon(i\xi)$ for different materials become small and, in some cases, there is a crossover where the inequality is no longer satisfied even if it was for lower frequencies. If this contribution to the force is small, this crossover is unimportant; however, if this crossover occurs at a low-enough frequency or results in a significant difference in $\varepsilon(i\xi)$ for frequencies higher than the crossover, the force may be significantly affected and cause a change in the sign with distance. This is a result of the fact that higher frequency contributions contribute more to short-range interactions and lower frequency contributions contribute more to long-range interactions. This type of behavior can be found, for example, with the combination of barium titanate and calcite immersed in ethanol, as described in [86].

D. Devices Based on Repulsive Casimir Forces

Repulsive Casimir–Lifshitz forces could be of significant interest technologically as this technique might be used to develop ultrasensitive force and torque sensors by counterbalancing gravity to levitate an object immersed in fluid above a surface without disturbing electric or magnetic interactions. Because the surfaces never come into direct contact as a result of their mutual repulsion, these objects are free to rotate or translate relative to each other with virtually no static friction. Dynamical damping due to viscosity will put limits on how quickly such a device can respond to changes in its surroundings; however, in principle, even the smallest translations or rotations can be detected on longer time scales. Thus, force and torque sensors could be developed that surpass those used currently. Fig. 9 shows an example of a QED floatation device: a nano-compass sensitive to very small static magnetic fields [87].

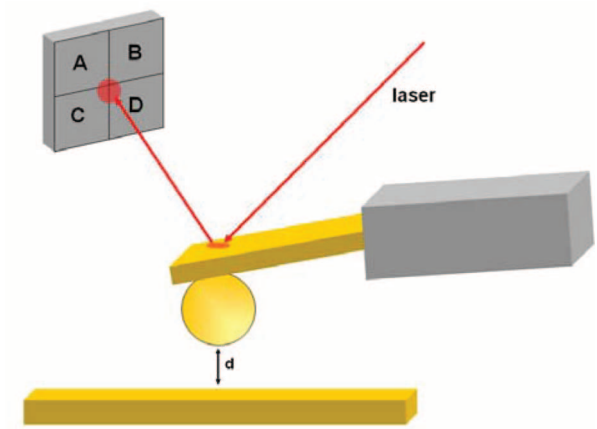

Fig. 10. Schematic setup for detecting the Casimir force via an AFM. A laser is reflected off the back of a microcantilever, on which a sphere is attached and metallized. The reflected beam is detected on a split quadrant photodetector, which monitors the cantilever's deflection caused by any vertical force.

E. AFM Measurement Technique

To measure attractive and repulsive Casimir–Lifshitz forces in fluids, a detection scheme using an AFM can be employed. Previous experiments have been performed using an AFM to measure close-range van der Waals forces in fluid (see, for example, [88]),[2] or the long-range Casimir force in vacuum [17]–[19]. By modification of these techniques, long-range interactions can be measured in fluidic environments.

A schematic of the typical AFM force apparatus is shown in Fig. 10. A large sphere (diameter between 50 and 200 μm) is attached, using a conductive epoxy, to a standard micro-cantilever used for contact mode imaging. The sphere and cantilever chip

[2]Indications of the existence of close-range (approximately a few nanometers) repulsive van der Waals forces have been reported in [83], [89], and [90].

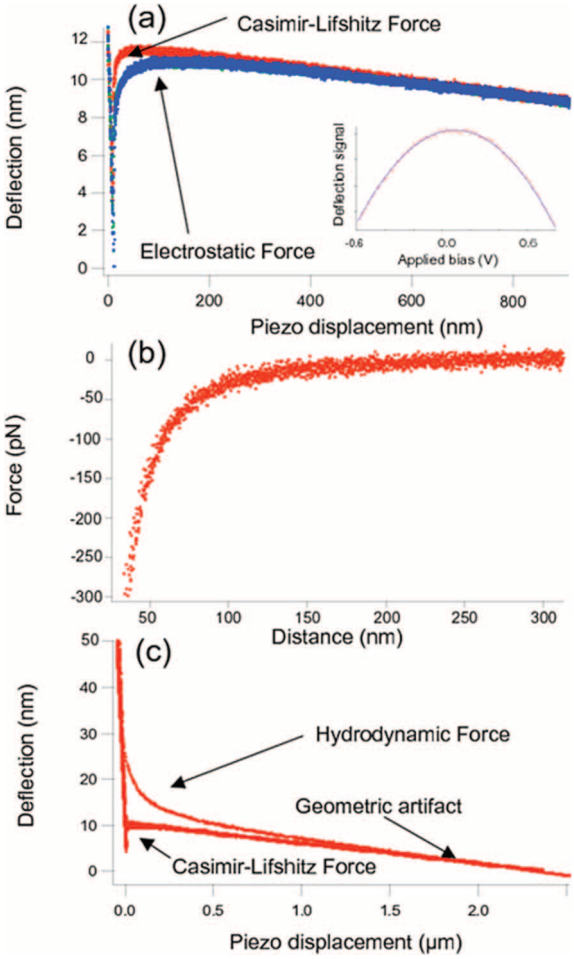

Fig. 11. Data and calibration procedures for determining the Casimir force interaction using an AFM. (a) Cantilever deflection measurements and electrostatic calibration procedure performed in air. Cantilever deflection as a function of voltage applied between the tip and the sample to determine the contact potential (*inset*). (b) Resulting Casimir force versus distance determined from the calibration procedure and measurements of (a). (c) Cantilever deflection measurements in ethanol using a hydrodynamic calibration. The linear slope, most visible at large piezo displacements, in (a) and (c) is an artifact due to laser deflection as described in the text.

are coated with a metallic layer and attached to a piezoelectric column to control vertical displacement from the surface of a plate (which is either metallic or dielectric). The extension of the piezoelectric column is detected via a linear variable differential transformer (LVDT), which is necessary for accurate detection of displacements to avoid nonlinearities and hysteresis inherent in piezoelectrics. A laser is projected onto the back of the cantilever and is reflected onto a four-quadrant photodetector. Vertical deflections of the cantilever can be detected by monitoring the difference signal between the top two quadrants and the bottom two quadrants of the detector. Calibration procedures are, then, used to convert the deflection difference signal into a force [17], [91]–[94].

For metal objects in air or vacuum, electrostatic forces can be used to determine the spring constant [17]. For this method, the plate is electrically grounded to the AFM while a voltage with respect to this ground is applied to the sphere. The electrostatic force between a sphere and a plate at separation d and electrostatic potential difference ΔV is

$$F_{\text{electrostatic}} = -\frac{\pi\varepsilon_o R}{d}\Delta V^2 \tag{7}$$

where ε_o is the vacuum permittivity. Fig. 11(a) shows the cantilever deflection versus piezo displacement for $\Delta V = 0$ and $\Delta V = \pm 200$ mV. It should be noted that a linear artifact that results from the curvature of the cantilever and the reflection of the laser is also present in Fig. 11(a) and (c). These effects, which are well known, are independent of the sphere–plate separation and are removed from the analysis. The resulting Casimir interaction, after calibration, is shown in Fig. 11(b) for a 50-μm-diameter sphere coated with gold above a gold-coated plate.

When measurements are made between materials (metals or dielectrics) in fluids, electrostatic interactions are greatly reduced by the intervening fluid. In this case, hydrodynamic forces can be used for calibration and determination of the cantilever spring constant [94]. The hydrodynamic force between a sphere and a plate is

$$F_{\text{hydrodynamic}} = \frac{6\pi\eta v}{d}R^2 \tag{8}$$

where η is the fluid viscosity and v is the velocity of the sphere in the direction of the plate. Fig. 11(c) shows the cantilever deflection as a function of piezo displacement for a 50-μm gold-coated sphere in ethanol above a gold plate moving with piezo velocities of 5 μm/s and 50 nm/s, where the former is used with (8) for calibration, and the latter is used to determine the Casimir force when the hydrodynamic drag is negligible (i.e., for slow piezo velocities). Future experiments will involve probing the Casimir–Lifshitz interaction between different materials in fluid.

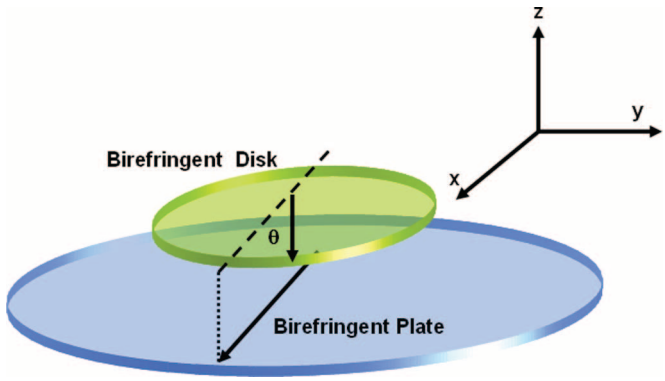

Fig. 12. QED torque develops between two birefringent parallel plates with in-plane optical axis when they are placed in close proximity.

IV. QED Torque

The effect of the zero-point energy between two optically anisotropic materials, as shown in Fig. 12, has also been considered [61], [62], [86], [95]–[100]. In this case, the fluctuating electromagnetic fields have boundary conditions that depend on the relative orientation of the optical axes of the materials; hence, the zero-point energy arising from these fields also has an angular dependence. This leads to a torque that tends to align

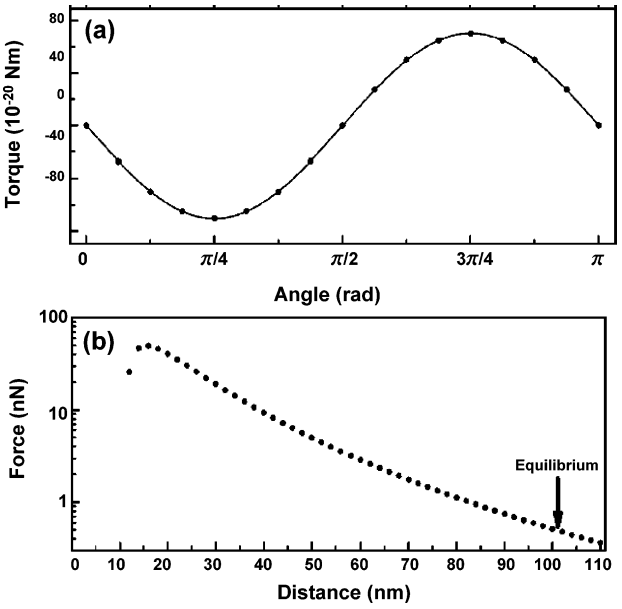

Fig. 13. (a) Calculated torque as a function of angle between a 40 μm diameter disk made of calcite and a barium titanate plate separated in vacuum by a distance $d = 100$ nm. The lines represent a fit with (9). (b) Calculated retarded van der Waals force as a function of plate separation for this system at a rotation angle of $\pi/4$. The *arrow* represents the distance at which the retarded van der Waals repulsion is in equilibrium with the weight of the disk.

two of the principal axes of the materials in order to minimize the system's energy. We have recently shown that such torques should, indeed, be measurable and have suggested experimental configurations to perform these measurements [86], [95].

In 1972, Parsegian and Weiss derived an expression for the short-range, nonretarded van der Waals interaction energy between two semi-infinite dielectrically anisotropic materials immersed within a third material [61]. This result, obtained by the summation of the electromagnetic surface mode fluctuations, showed that the interaction energy was inversely proportional to the separation squared and depended on the angle between the optical axes of the two anisotropic materials. In 1978, Barash independently derived an expression for the interaction energy between two anisotropic materials using the Helmholtz free energy of the electromagnetic modes, which included retardation effects [62]. In the nonretarded limit, Barash's expression confirmed the inverse square distance dependence of Parsegian and Weiss and that the torque, in this limit, varies as $\sin(2\theta)$, where θ is the angle between the optical axes of the materials.

The equations that govern the torque in the general case of arbitrary distances are quite cumbersome and are treated in detail elsewhere [62], [86]. For brevity, we refer the reader to those papers for a more in-depth analysis and simply state a few of the relevant results. First, the torque is proportional to the surface area of the interacting materials and decreases with increasing surface separation. Second, it is found that the QED torque at a given distance varies as

$$M = A \sin(2\theta) \tag{9}$$

even in the retarded limit, where A is the value of the torque at $\theta = \pi/4$. Fig. 13(a) shows the torque as a function of angle for a 40-μm-diameter calcite disk in vacuum above a barium titanate plate at a distance of $d = 100$ nm [86]. The circles correspond to the calculated values of the torque, while the solid line corresponds to a best fit with (9).

Experimentally, it is difficult to use large disks in close proximity, because at such small separations, tolerances in the parallelism of two large surfaces (tens of microns in diameter) are extremely tight; in addition, it is difficult to keep them free of dust and contaminants. If the vacuum is replaced by liquid ethanol, the torque remains of the same order of magnitude; however, the three materials (calcite, ethanol, and barium titanate) have dielectric functions that obey (6). This will result in a repulsive Casimir–Lifshitz force that will counterbalance the weight of the disk and allow it to float at a predetermined distance above the plate. For a 20-μm-thick calcite disk with a diameter of 40 μm above a barium titanate plate in ethanol, the equilibrium separation was calculated to be approximately 100 nm with a maximum torque of $\sim 4 \times 10^{-19}$N m [86], as shown in Fig. 13(b).

For the observation of the QED torque, it was suggested in [86] that the disk be rotated by $\theta = \pi/4$ by means of the transfer of angular momentum of light from a polarized beam. The laser could, then, be shuttered, and one would visually observe the rotation of the disk back to its minimum energy orientation. The amount of angular momentum transfer determines the initial value of the angle of rotation. After the laser beam is blocked, the disk can rotate either clockwise or counterclockwise back to the equilibrium position depending on the value of the initial angle, making it possible to verify the $\sin(2\theta)$ dependence of the torque. Procedures to minimize the effect of charges on the plates and other artifacts were also discussed [86].

An alternative scheme involving the statistical analysis of Brownian motion was recently described in [95]. For this situation, the disk size is reduced to the point that Brownian motion causes translation and rotation. When these rotations become comparable to the QED rotation, the disk will no longer rotate smoothly to its minimum energy configuration. Instead, the angle between the optical axes will fluctuate to sample all angles. The probability distribution for the observation of the angle θ between the two optical axes is

$$p(\theta) = p_o \exp\left[\frac{-U(\theta)}{k_B T}\right] \tag{10}$$

where $U(\theta)$ is the potential energy of the QED orientation interaction, i.e., the energy associated with the torque, $k_B T$ is the thermal energy, p_o is a normalization constant such that $\int p(\theta)\, d\theta = 1$. By observing the angle between the axes as a function of time, one can deduce the probability distribution via a histogram of the angular orientations, as shown in Fig. 14. This is similar to the determination of the potential energy as a function of distance in total internal reflection microscopy (TIRM) experiments for optically trapped spherical particles [101], [102].

To observe this effect, one needs to levitate a birefringent disk above a birefringent plate at short range and be able to detect the orientation of the axes. This can be done either by using a repulsive Casimir–Lifshitz force or a double-layer repulsion

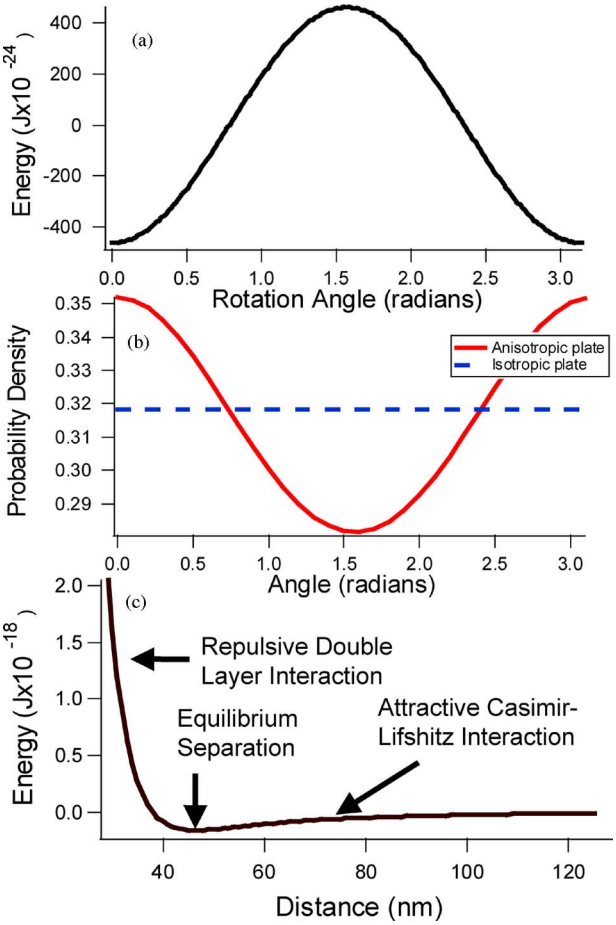

Fig. 14. QED interaction energies and probabilities. (a) Calculations of the angular dependence of the QED interaction energy between a 2-μm-diameter $LiNbO_3$ disk and a calcite plate. (b) Probability of detecting the rotation angle θ. (c) Energy as a function of separation between the disk and plate including contributions from the double layer interaction (dominant at close range), the Casimir–Lifshitz interaction (dominant at longer range), and gravity (negligible). Equilibrium is obtained around 50 nm.

force [46], [103] and video microscopy techniques [104] as described later.

The equilibrium separation occurs when the sum of the forces (Casimir–Lifshitz, double layer, and weight) acting on the particle is zero

$$\sum F = F_{\mathrm{CL}}(d) + D \times \exp\left[\frac{-d}{l}\right] - \pi R^2 h\, \Delta\rho g = 0 \quad (11)$$

where $F_{\mathrm{CL}}(d)$ is the Casimir–Lifshitz force at distance d, D is a constant related to the Poisson–Boltzmann potential evaluated at the surface due to charging, l is the Debye length, R is the radius of the disk, h is the thickness of the disk, $\Delta\rho$ is the density difference between the disk and the solution, and g is the acceleration due to gravity. Both the Casimir–Lifshitz force and the weight of the disks are set by the geometry of the system and the materials chosen; however, the double layer force can be modified by changing the electrolyte concentration. Thus, the floatation height can be adjusted in this way. Fig. 14(c) shows the approximate interaction energy following from the forces of (11), where we have chosen a double-layer interaction leading to a levitation height of approximately 50 nm, with deviations of a few nanometers due to thermal energy (k_BT), for a lithium niobate disk with radius $R = 1\mu$m and thickness $h = 0.5$ μm in an aqueous solution above a calcite plate.

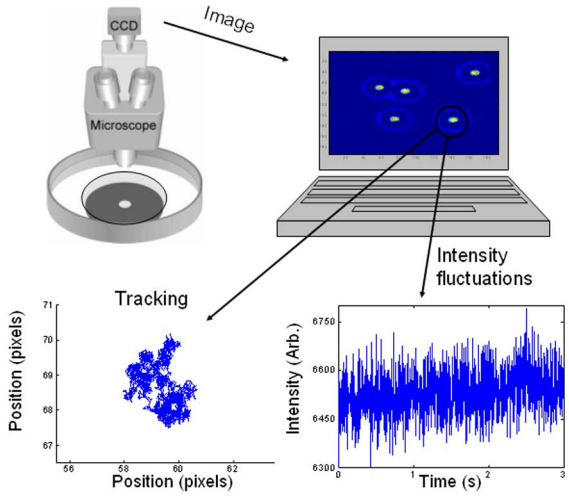

Fig. 15. Schematic of the Brownian motion detection scheme showing data for a non-birefringent spherical particle. Light is recorded via a CCD and digitized to allow for tracking and determination of intensity fluctuations.

In order to track the motion of the disk above the plate, a video microscopy setup similar to the one described in [104] is currently being used by the Harvard University group [95]. The disk's motion is tracked and recorded as is the intensity of the transmitted light. The orientation of the disk is determined by placing it between a combination of polarizing optical components so that the intensity of the transmitted light can be related to the orientation of the optical axis. In order to determine the expected optical intensity at the output as a function of θ, the Jones matrix representation of the optical elements is used to determine the exiting E-field from which the intensity is calculated [105], [106]. For suitably chosen optical components (see [95]), the intensity is proportional to $[1 - \cos(2\theta)]$. From a histogram of the intensities, we can, then, determine the preferred angular orientation of the disk and, hence, the angular QED interaction energy and the torque.

Fig. 15 shows the typical configuration for such experiments. The thermal fluctuations of the particles are recorded via a CCD camera attached to an upright microscope. The particles' centers can be determined and tracked by the method of [104] with a standard deviation of less than 1/10 pixel. Fig. 15 shows both the tracking and intensity fluctuations recorded for a spherical non-birefringent particle. For non-birefringent particles, the intensity fluctuations are due to scattering from imperfections within the particle as it undergoes Brownian motion. In order to study the QED torque, small birefringent disks should be used. Such disks have been fabricated using a combination of crystal ion slicing [107], mechanical polishing, and focused ion

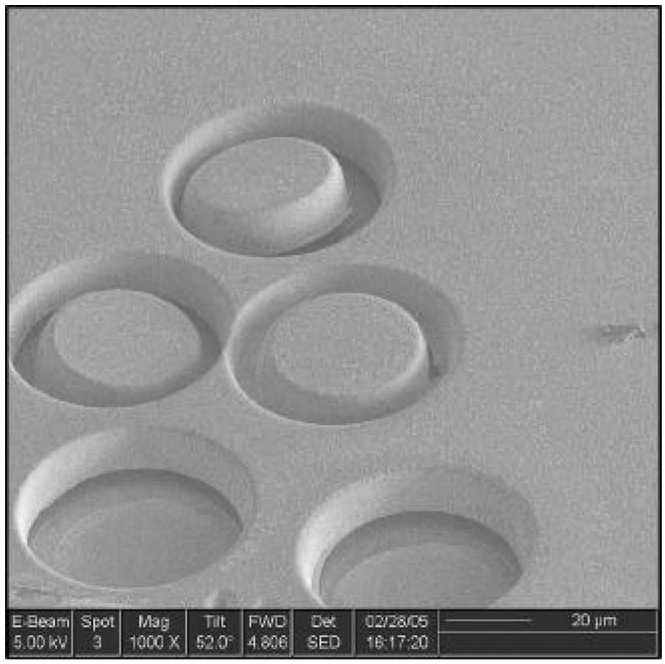

Fig. 16. $LiNbO_3$ disks fabricated by crystal ion slicing and FIB sculpting.

beam (FIB) sculpting, as shown in Fig. 16. To date, no experiments have been performed with birefringent particles; however, this detection scheme should be suitable for such QED torque experiments.

V. Future Directions

A number of other interesting QED phenomena await experimental investigation.

A. Phase Transitions and the Casimir Effect

The Harvard group has initiated a study of the influence of phase transitions on the Casimir force. The geometry is that of the sphere and plate as discussed in previous sections. The sphere is coated by thick gold while the plate consists of materials such as Bi–Sr–Ca–Cu–O (BSSCO) that exhibit high-temperature superconductivity. This material can be easily cleaved, giving atomically flat surfaces, which will greatly reduce uncertainties due to surface roughness. The Casimir effect will be measured below and above the transition temperature. Recently, the influence of Casimir energy on the critical field of a superconducting film has been theoretically investigated, and it was shown that it might be possible to directly measure the variation of Casimir energy that accompanies the superconducting transition [108].

B. Nonadditivity of Casimir Forces

Unlike many forces, the Casimir force is nonadditive in that the force between two macroscopic bodies cannot be obtained by pairwise summation of the interacting molecular interactions [9]. That is, the retarded Casimir–Polder force [109] between two molecules is influenced by the presence of a third molecule due to the electromagnetic nature of this interaction. The effect of nonadditivity greatly complicates predictions of the Casimir force for nonstandard geometries, such as corrugations, when perturbative methods are not applicable [110]. Experimental investigations of the nonadditive nature of the Casimir force between surfaces comprising a variety of materials and geometries is, therefore, of significant interest.

C. Casimir Friction

There has been an interesting prediction that dissipative retarded van der Waals forces can arise between surfaces in relative motion due to the exchange of virtual photons that couple to acoustic phonons in the material [111]. Similar dissipative Casimir forces can arise between metals; here, virtual photons would couple to particle–hole excitations in the metal [112]. This would lead to changes with position of the Q of suitable MEMS oscillators, such as the ones described in Section II-A.

Pendry has considered another type of vacuum friction when two perfectly smooth featureless surfaces at $T = 0$, defined only by their respective dielectric functions, separated by a finite distance, move parallel to each other [113]. He found large frictional effects comparable to everyday frictional forces provided that the materials have resistivities of the order of 1 MΩ and that the surfaces are in close proximity. The friction depends solely on the reflection coefficients of the surfaces for electromagnetic waves, and its detailed behavior with shear velocity and separation is controlled by the dispersion of the reflectivity with frequency. There exists a potentially rich variety of vacuum friction effects, as discussed in a recent article [114].

D. Dynamic Casimir Effect

It is also interesting to point out that the nonuniform relative acceleration of the metal and the sphere will lead, at least in principle, in the Casimir oscillator of Section II-A to an additional damping mechanism associated with the parametric down-conversion of vibrational quanta into pairs of photons, a QED effect associated with the nonlinear properties of vacuum. This phenomenon, which was investigated theoretically by Lambrecht *et al*. in the context of a vibrating parallel plate capacitor [115], is an example of the so-called dynamical Casimir effect, i.e., the nonthermal radiation emitted by uncharged metal or dielectric bodies in a state of nonuniform acceleration [116]. The extraction of photons from vacuum in a cavity vibrating at twice the fundamental frequency of the cavity can be viewed as a parametric "vacuum squeezing" phenomenon. Physically, photons are created as a result of the time-dependent boundary conditions of cavity modes, which produce electromagnetic fields. The observation of this effect would require a very high cavity $Q(\sim 10^8$–$10^9)$ typical of superconductive cavities and gigahertz oscillations frequencies [115]. Such frequencies have been achieved in NEMS [117].

It is worth pointing out that radiation can be extracted from QED fluctuations also from a beam of neutral molecules interacting with a grating. In this case, coherent radiation can be generated as result of the time-dependent modulation of the Casimir–Polder–van der Waals force between the molecules

and the grating. Radiation in the far infrared region should be attainable with beam densities of 10^{17}cm^{-3} [118].

VI. Conclusion

In conclusion, following a comprehensive state-of-the-art overview of the Casimir effect from its original proposal, we have discussed our recent and ongoing research in this promising field.

Acknowledgment

The authors would like to thank M. Lisanti, L. Spector, M. B. Romanowsky, N. Geisse, K. Parker, R. M. Osgood, R. Roth, H. Stone, Y. Barash, V. A. Aksyuk, R. N. Kleinman, and D. J. Bishop for their collaborations and R. Guerra, R. Onofrio, M. Kardar, R. L. Jaffe, S. G. Johnson, J. D. Joannopoulos, L. Levitov, V. Parsegian, J. N. Israelachvili, E. Tosatti, V. Pogrovski, M. Scully, P. W. Milonni, W. Kohn, M. Cohen, A. Lambrecht, F. Intravaia, and S. Reynaud for helpful suggestions and discussions.

References

[1] K. L. Ekinci and M. L. Roukes, "Nanoelectromechanical systems," *Rev. Sci. Instrum.*, vol. 76, pp. 061101-1–061101-12, 2005.

[2] K. C. Schwab and M. L. Roukes, "Putting mechanics into quantum mechanics," *Phys. Today*, vol. 58, pp. 36–42, Jul. 2005.

[3] M. L. Roukes, "Plenty of room indeed," *Sci. Amer.*, vol. 285, pp. 48–57, Sep. 2001.

[4] A. N. Cleland and M. L. Roukes, "A nanometer-scale mechanical electrometer," *Nature*, vol. 392, pp. 160–162, 1998.

[5] K. Schwab, E. A. Henriksen, J. M. Worlock, and M. L. Roukes, "Measurement of the quantum of thermal conductance," *Nature*, vol. 404, pp. 974–977, 2000.

[6] M. D. LaHaye, O. Buu, B. Camarota, and K. C. Schwab, "Approaching the quantum limit of a nanomechanical resonator," *Science*, vol. 304, pp. 74–77, 2004.

[7] A. Naik, O. Buu, M. D. LaHaye, A. D. Armour, A. A. Clerk, M. P. Blencowe, and K. C. Schwab, "Cooling a nanomechanical resonator with quantum back-action," *Nature*, vol. 443, pp. 193–196, 2006.

[8] A. N. Cleland and M. R. Geller, "Mechanical quantum resonators," in *Electron. Properties of Novel Nanostructures,* H. Kuzmany, Ed. *AIP Conf. Proc.*, 2005, vol. 786, pp. 396–400.

[9] P. W. Milonni, *The Quantum Vacuum: An Introduction to Quantum Electrodynamics*. San Diego, CA: Academic, 1993.

[10] H. B. G. Casimir, "On the attraction between two perfectly conducting plates," *Proc. K. Ned. Akad. Wet.*, vol. 60, pp. 793–795, 1948.

[11] ——, *Haphazard Reality. Half a Century of Science*. New York: Harper and Row, 1983.

[12] R. L. Jaffe and A. Scardicchio, "Casimir effect and geometric optics," *Phys. Rev. Lett.*, vol. 92, pp. 070402-1–070402-5, 2004.

[13] A. Scardicchio and R. L. Jaffe, "Casimir effects: An optical approach. I: Foundations and examples," *Nucl. Phys. B*, vol. 704, pp. 552–582, 2005.

[14] M. J. Sparnaay, "Measurements of attractive forces between flat plates," *Physica*, vol. 24, pp. 751–764, 1958.

[15] P. H. G. M. van Blokland and J. T. G. Overbeek, "Van der Waals forces between objects covered with a chromium layer," *J. Chem. Soc., Faraday Trans.*, vol. 74, pp. 2637–2651, 1978.

[16] S. K. Lamoreaux, "Demonstration of the Casimir force in the 0.6 to 6 μm range," *Phys. Rev. Lett.*, vol. 78, pp. 5–8, 1997.

[17] U. Mohideen and A. Roy, "Precision measurement of the Casimir force from 0.1 to 0.9 mm," *Phys. Rev. Lett.*, vol. 81, pp. 4549–4552, 1998.

[18] A. Roy, C.-Y. Lin, and U. Mohideen, "Improved precision measurement of the Casimir force," *Phys. Rev. D*, vol. 60, pp. 111101-1–111101-5, 1999.

[19] B. W. Harris, F. Chen, and U. Mohideen, "Precision measurement of the Casimir force using gold surfaces," *Phys. Rev. A*, vol. 62, pp. 052109-1–052109-5, 2000.

[20] T. Ederth, "Template-stripped gold surfaces with 0.4-nm rms roughness suitable for force measurements: Application to the Casimir force in the 20–100 nm range," *Phys. Rev. A*, vol. 62, pp. 062104-1–062104-8, 2000.

[21] G. Bressi, G. Carugno, R. Onofrio, and G. Ruoso, "Measurement of the Casimir force between parallel metallic surfaces," *Phys. Rev. Lett.*, vol. 88, pp. 041804-1–041804-4, 2002.

[22] R. S. Decca, D. Lopez, E. Fischbach, and D. E. Krause, "Measurement of the Casimir force between dissimilar metals," *Phys. Rev. Lett.*, vol. 91, pp. 050402-1–050402-4, 2003.

[23] R. S. Decca, D. Lopez, E. Fischbach, G. L. Klimchitskaya, D. E. Krause, and V. M. Mostepanenko, "Precise comparison of theory and new experiment for the Casimir force leads to stronger constraints on thermal quantum effects and long-range interactions," *Ann. Phys.*, vol. 318, pp. 37–80, 2005.

[24] H. B. Chan, V. A. Aksyuk, R. N. Kleinman, D. J. Bishop, and F. Capasso, "Quantum mechanical actuation of microelectromechanical systems by the Casimir force," *Science*, vol. 291, pp. 1941–1944, 2001.

[25] B. V. Derjaguin and I. I. Abrikosova, "Direct measurement of the molecular attraction of solid bodies. Statement of the problem and measurement of the force by using negative feedback," *Sov. Phys. JETP*, vol. 3, pp. 819–829, 1957.

[26] P. W. Milonni and M.-L. Shih, "Casimir forces," *Contemp. Phys.*, vol. 33, no. 5, pp. 313–322, 1992.

[27] L. Spruch, "Long-range (Casimir) interactions," *Science*, vol. 272, pp. 1452–1455, 1996.

[28] V. A. Parsegian, *Van der Waals Forces: A Handbook for Biologists, Chemists, Engineers, and Physicists*. New York: Cambridge University Press, 2006.

[29] V. M. Mostepanenko and N. N. Trunov, *The Casimir Effect and its Applications*. Oxford, U.K.: Oxford Univ. Press, 1997.

[30] K. A. Milton, *The Casimir Effect: Physical Manifestations of Zero-Point Energy*. Singapore: World Scientific, 2001.

[31] M. Bordag, U. Mohideen, and V. M. Mostepanenko, "New developments in the Casimir effect," *Phys. Rep.*, vol. 353, pp. 1–205, 2001.

[32] P. A. Martin and P. R. Buenzli, "The Casimir effect," *Acta Phys. Polon. B*, vol. 37, pp. 2503–2559, 2006.

[33] A. Lambrecht, "The Casimir effect: A force from nothing," *Phys. World*, vol. 15, pp. 29–32, Sep. 2002.

[34] S. K. Lamoreaux, "Resource letter CF-1: Casimir force," *Amer. J. Phys.*, vol. 67, no. 10, pp. 850–861, Oct. 1999.

[35] E. M. Lifshitz, "The theory of molecular attractive forces between solids," *Sov. Phys. JETP*, vol. 2, pp. 73–83, 1956.

[36] I. E. Dzyaloshinskii, E. M. Lifshitz, and L. P. Pitaevskii, "The general theory of van der Waals forces," *Adv. Phys.*, vol. 10, pp. 165–209, 1961.

[37] A. Lambrecht and S. Reynaud, "Casimir force between metallic mirrors," *Eur. Phys. J. D*, vol. 8, pp. 309–318, 2000.

[38] G. L. Klimchitskaya, U. Mohideen, and V. M. Mostepanenko, "Casimir and van der Waals forces between two plates or a sphere (lens) above a plate made of real metals," *Phys. Rev. A*, vol. 61, pp. 062107-1–062107-12, 2000.

[39] E. D. Palik, Ed., *Handbook of Optical Constants of Solids*. New York: Academic, 1998.

[40] ——, in *Handbook of Optical Constants of Solids: II*, E. D. Palik, Ed. New York: Academic, 1991.

[41] M. A. Ordal, R. J. Bell, R. W. Alexander, Jr., L. L. Long, and M. R. Querry, "Optical properties of fourteen metals in the infrared and far infrared: Al, Co, Cu, Au, Fe, Pb, Mo, Ni, Pd, Pt, Ag, Ti, V, and W," *Appl. Opt.*, vol. 24, pp. 4493–4499, 1985.

[42] A. A. Maradudin and P. Mazur, "Effects of surface roughness on the van der Waals force between macroscopic bodies," *Phys. Rev. B*, vol. 22, pp. 1677–1686, 1980.

[43] V. B. Bezerra, G. L. Klimchitskaya, and C. Romero, "Casimir force between a flat plate and a spherical lens: Application to the results of a new experiment," *Mod. Phys. Lett. A*, vol. 12, pp. 2613–2622, 1997.

[44] P. A. M. Neto, A. Lambrecht, and S. Reynaud, "Roughness correction to the Casimir force: Beyond the proximity force approximation," *Europhys. Lett.*, vol. 69, pp. 924–930, 2005.

[45] J. Mahanty and B. W. Ninham, *Dispersion Forces*. London, U.K.: Academic, 1976.

[46] J. N. Israelachvili, *Intermolecular and Surface Forces*. London, U.K.: Academic, 1991.

[47] C. Henkel, K. Joulain, J. Ph. Mulet, and J.-J. Greffet, "Coupled surface polaritons and the Casimir force," *Phys. Rev. A*, vol. 69, pp. 023808-1–023808-7, 2004.

[48] F. Intravaia and A. Lambrecht, "Surface plasmon modes and the Casimir energy," *Phys. Rev. Lett.*, vol. 94, pp. 110404-1–110404-4, 2005.

[49] F. Intravaia, "Effet Casimir et interaction entre plasmons de surface," Ph.D. dissertation, Univ. Paris, Paris, France, 2005.

[50] S. K. Lamoreaux, "Comment on 'precision measurement of the Casimir force from 01 to 0.9 μm'," *Phys. Rev. Lett.*, vol. 83, p. 3340, 1999.

[51] ——, "Calculation of the Casimir force between imperfectly conducting plates," *Phys. Rev. A*, vol. 59, pp. 3149–3153, 1999.

[52] D. Iannuzzi, I. Gelfand, M. Lisanti, and F. Capasso, New Challenges and directions in Casimir force experiments*Proc. 6th Workshop Quantum Field Theory Under Influence External Conditions*. Paramus, NJ, Rinton, 2004, pp. 11–16.

[53] I. Pirozhenko, A. Lambrecht, and V. B. Svetovoy, "Sample dependence of the Casimir force," *N. J. Phys.*, vol. 8, p. 238, 2006.

[54] E. Buks and M. L. Roukes, "Metastability and the Casimir effect in micromechanical systems," *Europhys. Lett.*, vol. 54, no. 2, pp. 220–226, Apr. 2001.

[55] H. B. Chan, V. A. Aksyuk, R. N. Kleinman, D. J. Bishop, and F. Capasso, "Nonlinear micromechanical Casimir oscillator," *Phys. Rev. Lett.*, vol. 87, pp. 211801-1–211801-4, 2001.

[56] D. Iannuzzi, M. Lisanti, J. N. Munday, and F. Capasso, "The design of long range quantum electrodynamical forces and torques between macroscopic bodies," *Solid State Commun.*, vol. 135, pp. 618–626, 2005.

[57] M. Lisanti, D. Iannuzzi, and F. Capasso, "Observation of the skin-depth effect on the Casimir force between metallic surfaces," *Proc. Natl. Acad. Sci. USA*, vol. 102, pp. 11989–11992, 2005.

[58] R. Golestanian and M. Kardar, "Mechanical response of vacuum," *Phys. Rev. Lett.*, vol. 78, pp. 3421–3425, 1997.

[59] ——, "Path-integral approach to the dynamic Casimir effect with fluctuating boundaries," *Phys. Rev. A*, vol. 58, pp. 1713–1722, 1998.

[60] T. Emig, A. Hanke, and M. Kardar, "Probing the strong boundary shape dependence of the Casimir force," *Phys. Rev. Lett.*, vol. 87, pp. 260402-1–26040-4, 2001.

[61] V. A. Parsegian and G. H. Weiss, "Dielectric anisotropy and the van der Waals interaction between bulk media," *J. Adhes.*, vol. 3, pp. 259–267, 1972.

[62] Y. Barash, "On the moment of van der Waals forces between anisotropic bodies," *Izv. Vyssh. Uchebn. Zaved. Radiofiz.*, vol. 12, pp. 1637–1643, 1978.

[63] S. D. Senturia, *Microsystem Design*. Norwell, MA: Kluwer, 2001.

[64] D. J. Bishop, C. R. Giles, and G. P. Austin, "The Lucent lambdarouter MEMS technology of the future here today," *IEEE Commun. Mag.*, vol. 40, no. 3, pp. 75–79, Mar. 2002.

[65] V. A. Aksyuk, F. Pardo, D. Carr, D. Greywall, H. B. Chan, M. E. Simon, A. Gasparyan, H. Shea, V. Lifton, C. Bolle, S. Arney, R. Frahm, M. Paczkowski, M. Haueis, R. Ryf, D. T. Neilson, J. Kim, C. R. Giles, and D. Bishop, "Beam-steering micromirrors for large optical cross-connects," *J. Lightw. Technol.*, vol. 21, no. 3, pp. 634–642, Mar. 2003.

[66] M. Serry, D. Walliser, and J. Maclay, "The role of the Casimir effect in the static deflection and stiction of membrane strips in microelectromechanical systems (MEMS)," *J. Appl. Phys.*, vol. 84, pp. 2501–2506, 1998.

[67] H. J. De Los Santos, "Nanoelectromechanical quantum circuits and systems," *Proc. IEEE*, vol. 91, no. 11, pp. 1907–1921, Nov. 2003.

[68] D. Iannuzzi, M. Lisanti, and F. Capasso, "Effect of hydrogen-switchable mirrors on the Casimir force," *Proc. Natl. Acad. Sci. USA*, vol. 101, pp. 4019–4023, 2004.

[69] F. M. Serry, D. Walliser, and G. J. Maclay, "The anharmonic Casimir oscillator (ACO)—The Casimir effect in a model microelectromechanical system," *J. Microelectromech. Syst.*, vol. 4, pp. 193–205, 1995.

[70] L. D. Landau and E. M. Lifshitz, *Mechanics*. New York: Pergamon, 1976.

[71] D. Iannuzzi, M. Lisanti, J. N. Munday, and F. Capasso, "Quantum fluctuations in the presence of thin metallic films and anisotropic materials," *J. Phys. A: Math. Gen.*, vol. 39, pp. 6445–6454, 2006.

[72] D. B. Hough and L. R. White, "The calculation of Hamaker constants from Lifshitz theory with applications to wetting phenomena," *Adv. Colloid Interface Sci.*, vol. 14, pp. 3–41, 1980.

[73] J. N. Huiberts, R. Griessen, J. H. Rector, R. J. Wijngaarden, J. P. Dekker, D. G. de Groot, and N. J. Koeman, "Yttrium and lanthanum hydride films with switchable optical properties," *Nature*, vol. 380, pp. 231–234, 1996.

[74] T. J. Richardson, J. L. Slack, R. D. Armitage, R. Kostecki, B. Farangis, and M. D. Rubin, "Switchable mirrors based on nickel–magnesium films," *Appl. Phys. Lett.*, vol. 78, pp. 3047–3049, 2001.

[75] S. de Man and D. Iannuzzi, "On the use of hydrogen switchable mirrors in Casimir force experiments," *N. J. Phys.*, vol. 8, p. 235, 2006.

[76] T. H. Boyer, "Quantum electromagnetic zero-point energy of a conducting spherical shell and the Casimir model for a charged particle," *Phys. Rev.*, vol. 174, pp. 1764–1776, 1968.

[77] J. Ambjorn and S. Wolfram, "Properties of the vacuum. I. Mechanical and thermodynamic," *Ann. Phys.*, vol. 147, pp. 1–32, 1983.

[78] G. J. Maclay, "Analysis of zero-point electromagnetic energy and Casimir forces in conducting rectangular cavities," *Phys. Rev. A*, vol. 61, pp. 052110-1–052110-18, 2000.

[79] N. Graham, R. L. Jaffe, V. Khemani, M. Quandt, O. Schroeder, and H. Weigel, "The Dirichlet Casimir problem," *Nucl. Phys. B*, vol. 677, pp. 379–404, 2004.

[80] M. P. Hertzberg, R. L. Jaffe, M. Kardar, and A. Scardicchio, "Attractive Casimir forces in a closed geometry," *Phys. Rev. Lett.*, vol. 95, pp. 250402-1–250402-4, 2005.

[81] U. Tartaglino, T. Zykova Timan, F. Ercolessi, and E. Tosatti, "Melting and nonmelting of solid surfaces and nanosystems," *Phys. Rep.*, vol. 411, pp. 291–321, 2005.

[82] H. C. Hamaker, "The London–van der Waals physical attraction between spherical particles," *Physica*, vol. 4, pp. 1058–1072, 1937.

[83] S. Lee and W. M. Sigmund, "Repulsive van der Waals forces for silica and alumina," *J. Colloid Interface Sci.*, vol. 243, pp. 365–369, 2001.

[84] H. F. Mark, D. F. Othmer, C. G. Overberger, and G. T. Seaborg, Eds., *Encyclopedia of Chemical Technology*. New York: Wiley, 1980.

[85] L. Bergstrom, "Hamaker constants of inorganic materials," *Adv. Colloid Interface Sci.*, vol. 70, pp. 125–169, 1997.

[86] J. N. Munday, D. Iannuzzi, Y. Barash, and F. Capasso, "Torque on birefringent plates induced by quantum fluctuations," *Phys. Rev. A*, vol. 71, pp. 042102-1–042102-9, 2005.

[87] D. Iannuzzi, J. Munday, and F. Capasso, "Ultra-low static friction configuration," Patent submitted, 2005.

[88] W. A. Ducker, T. J. Senden, and R. M. Pashley, "Direct force measurements of colloidal forces using an atomic force microscope," *Nature*, vol. 353, pp. 239–241, 1991.

[89] A. Milling, P. Mulvaney, and I. Larson, "Direct measurement of repulsive van der Waals interactions using an atomic force microscope," *J. Colloid Interface Sci.*, vol. 180, pp. 460–465, 1996.

[90] A. Meurk, P. F. Luckham, and L. Bergstrom, "Direct measurement of repulsive and attractive van der Waals forces between inorganic materials," *Langmuir*, vol. 13, pp. 3896–3899, 1997.

[91] J. P. Cleveland, S. Manne, D. Bocek, and P. K. Hansma, "A nondestructive method for determining the spring constant of cantilevers for scanning force microscopy," *Rev. Sci. Instrum.*, vol. 64, no. 2, pp. 403–405, Feb. 1993.

[92] J. E. Sader, J. W. M. Chon, and P. Mulvaney, "Calibration of rectangular atomic force microscope cantilevers," *Rev. Sci. Instrum.*, vol. 70, no. 10, pp. 3967–3969, Oct. 1999.

[93] J. L. Hutter and J. Bechhoefer "Calibration of atomic-force microscope tips," *Rev. Sci. Instrum.*, vol. 64, no. 7, pp. 1868–1873, Jul. 1993.

[94] V. S. J. Craig and C. Neto, "In situ calibration of colloid probe cantilevers in force microscopy: Hydrodynamic drag on a sphere approaching a wall," *Langmuir*, vol. 17, pp. 6018–6022, 2001.

[95] J. N. Munday, D. Iannuzzi, and F. Capasso, "Quantum electrodynamical torques in the presence of Brownian motion," *N. J. Phys.*, vol. 8, p. 244, 2006.

[96] S. J. van Enk, "Casimir torque between dielectrics," *Phys. Rev. A*, vol. 52, pp. 2569–2575, 1995.

[97] O. Kenneth and S. Nussinov, "New 'polarized version' of the Casimir effect is measurable," *Phys. Rev. D*, vol. 63, pp. 121701-1–121701-5, 2001.

[98] S. C. G. Shao, A. H. Tong, and J. Luo, "Casimir torque between two birefringent plates," *Phys. Rev. A*, vol. 72, pp. 022102-1–022102-5, 2005.

[99] J. C. Torres-Guzmán and W. L. Mochán, "Casimir torque," *J. Phys. A: Math. Gen.*, vol. 39, pp. 6791–6798, 2006.

[100] R. B. Rodrigues, P. A. M. Neto, A. Lambrecht, and S. Reynaud, "Vacuum-induced torque between corrugated metallic plates," *Europhys. Lett.,* vol. 76, pp. 822–828, 2006.

[101] D. C. Prieve and N. A. Frej, "Total internal reflection microscopy: A quantitative tool for the measurement of colloidal forces," *Langmuir*, vol. 6, pp. 396–403, 1990.

[102] D. C. Prieve, "Measurement of colloidal forces with TIRM," *Adv. Colloid Interface Sci.*, vol. 82, pp. 93–125, 1999.

[103] W. B. Russel, D. A. Saville, and W. R. Schowalter, *Colloidal Dispersions*. Cambridge, U.K.: Cambridge Univ. Press, 1989.
[104] J. C. Crocker and D. G. Grier, "Methods of digital video microscopy for colloidal studies," *J. Colloid Interface Sci*., vol. 179, pp. 298–310, 1996.
[105] R. C. Jones, "New calculus for the treatment of optical systems. I. Description and discussion of the calculus," *J. Opt. A*., vol. 31, pp. 488–493, 1941.
[106] G. R. Fowles, *Introduction to Modern Optics*. New York: Dover, 1968.
[107] M. Levy, R. M. Osgood, R. Liu, L. E. Cross, G. S. Cargill, III, A. Kumar, and H. Bakhru, "Fabrication of single-crystal lithium niobate films by crystal ion slicing," *Appl. Phys. Lett*., vol. 73, pp. 2293–2295, 1998.
[108] G. Bimonte, E. Calloni, G. Esposito, and L. Rosa, "Casimir energy and the superconducting phase transition," *J. Phys. A: Math. Gen*., vol. 39, pp. 6161–6171, 2006.
[109] H. B. G. Casimir and D. Polder, "The influence of retardation on the London–van der Waals forces," *Phys. Rev*., vol. 73, pp. 360–372, 1948.
[110] R. Buscher and T. Emig, "Geometry and spectrum of Casimir forces," *Phys. Rev. Lett*., vol. 94, pp. 133901-1–133901-4, 2005.
[111] L. S. Levitov, "Van der Waals' friction," *Europhys. Lett*., vol. 8, pp. 499–504, 1989.
[112] ——, private communication, 2001.
[113] J. B. Pendry, "Shearing the vacuum–quantum friction," *J. Phys.: Condens. Matter*, vol. 9, pp. 10301–10320, 1997.
[114] M. Kardar and R. Golestanian, "The 'friction' of vacuum, and other fluctuation-induced forces," *Rev. Mod. Phys*., vol. 71, pp. 1233–1245, 1999.
[115] A. Lambrecht, M. Jaekel, and S. Reynaud, "Motion induced radiation from a vibrating cavity," *Phys. Rev. Lett*., vol. 77, pp. 615–618, 1996.
[116] J. Schwinger, "Casimir light: A glimpse," *Proc. Natl. Acad. Sci. USA*, vol. 90, pp. 958–959, 1993.
[117] X. M. H. Huang, X. L. Feng, C. A. Zorman, M. Mehregany, and M. L. Roukes, "VHF, UHF and microwave frequency nanomechanical resonators," *N. J. Phys*., vol. 7, p. 247, 2005.
[118] A. Belyanin, V. Kocharovsky, V. Kocharovsky, and F. Capasso, "Coherent radiation from neutral molecules moving above a grating," *Phys. Rev. Lett*., vol. 88, pp. 053602-1–053602-4, 2002.

Federico Capasso (M'79–SM'85–F'87) received the Doctor of Physics degree (*summa cum laude*) from the University of Rome, Rome, Italy, in 1973.

From 1974 to 1976, he was a Researcher at Fondazione Ugo Bordoni. He joined Bell Laboratories in 1976, where he held positions of a Member of Technical Staff (1977–1986), Department Head (1986–2000), and Vice President for Physical Research (2000–2002). In 1997, he was made a Bell Labs Fellow for his scientific contributions. He is currently the Robert Wallace Professor of Applied Physics and Vinton Hayes Senior Research Fellow in Electrical Engineering at Harvard University. He has been engaged in basic and applied research on the quantum design of new artificial materials and devices, known as bandstructure engineering, and also in investigations of the Casimir effect and of the field of surface plasmon photonics, which have opened up new directions in electronics, photonics, mesoscopic physics, and nanotechnology. He is a co-inventor of the quantum cascade laser, a fundamentally new light source, which has now been commercialized. More recently, he initiated a new line of research using MEMS to investigate the basic physics of the Casimir effect and its applications to nanomechanics. He has coauthored over 300 papers, edited four volumes, and holds over 40 U.S. patents.

Prof. Capasso is a member of the National Academy of Sciences, the National Academy of Engineering, and the American Academy of Arts and Sciences. His awards include the King Faisal International Prize for Science, the IEEE Edison Medal, the Arthur Schawlow Prize in Laser Science, the Wetherill Medal of the Franklin Institute, the Robert Wood Prize of the Optical Society of America (OSA), the William Streifer Award of the Laser and Electro-Optic Society (IEEE), the Rank Prize in Optoelectronics (U.K.), the IEEE David Sarnoff Award in Electronics, the Duddell Medal of the Institute of Physics (U.K.), the Willis Lamb Medal for Laser Science and Quantum Optics, the Materials Research Society Medal, the "Vinci of Excellence" Prize (France), the Welker Memorial Medal (Germany), the New York Academy of Sciences Award, the Newcomb Cleveland Prize of the American Association for the Advancement of Science. He is a Fellow of the Optical Society of America, the American Physical Society, the International Society for Optical Engineering (SPIE), and the American Association for the Advancement of Science (AAAS).

Jeremy N. Munday received the B.S. degree in physics and astronomy from Middle Tennessee State University, Murfreesboro, in 2003, and the M.A. degree in physics in 2005 from Harvard University, Cambridge, MA, where he is currently working toward the Ph.D. degree in the Department of Physics.

His current research interests include the Casimir effect and related quantum electrodynamical phenomena (e.g., torques arising from vacuum fluctuations), and engineering acoustic and electromagnetic materials for negative refraction, negative group delays, etc.

Mr. Munday is a member of Sigma Pi Sigma and the American Physical Society. He is also the recipient of the National Science Foundation Fellowship.

Davide Iannuzzi (M'06) received the Ph.D. degree in physics from the University of Pavia, Pavia, Italy, in 2002.

In 2001, he joined Bell Laboratories, Lucent Technologies, as a Postdoctoral Fellow. In 2003, he moved to Harvard University as a Postdoctoral Fellow. Since June 2005, he has been the Leader of a research group at Vrije Universiteit, Amsterdam, The Netherlands. His current research interests include the Casimir effect and the development of conceptually new micromachined devices.

Dr. Iannuzzi is a member of the American Physical Society, the European Physical Society, the Italian Physical Society, the Dutch Physical Society, and the Optical Society of America. In 2004, he received the VIDI Fellowship from the Netherlands Organization for Scientific Research, and in 2006, the Rhenaphotonics Alsace Best Design Award and the Rhenaphotonics Alsace Best Technology Award for his invention "fiber-top cantilever."

H. B. Chan received the Ph.D. degree in physics from Massachusetts Institute of Technology, Cambridge, in 1999.

From 1999 to 2000, he was Postdoctoral Member of Technical Staff at Bell Laboratories-Lucent Technologies, where he was also a Member of the Technical Staff from 2000 to 2003. Since 2004, he has been an Assistant Professor in the Department of Physics, University of Florida, Gainesville. His current research interests include microelectromechanical systems, Casimir forces, fluctuations in nonlinear systems, and optical properties of subwavelength metallic structures.